Acta Mechanica 105, 133–141 (1994)

ACTA MECHANICA

Theoretical analysis on mixed convection boundary layer flow over a wedge with uniform suction or injection

T. Watanabe, K. Funazaki, and **H. Taniguchi,** Morioka, Japan

(Received September 30, 1992; revised February 23, 1993)

Summary. Forced and free mixed convection boundary layer flow over a wedge with uniform suction or injection is theoretically investigated. Nonsimilar partial differential equations are transformed into ordinary differential equations by means of difference-differential method. The solutions of the resulting equations are obtained in integral forms and are calculated by iterative numerical procedures. The results were given for velocity profiles, temperature profiles, friction and heat transfer parameters for various values of suction/injection parameter, pressure gradient parameter and buoyancy parameter.

1 Introduction

The problem dealing with forced and free mixed convection flow past heated or cooled bodies with suction or injection is of interest in relation to boundary layer control. The forced and free mixed convection flow has been studied by many investigators [1]–[6], and the nonsimilar boundary layer equations were solved by using the weighting function method [7], the two-point finite difference method [8] and the difference-differential method [9].

In the present paper, the effect of uniform suction or injection on mixed convection boundary layer flow along a wedge is theoretically analysed. The nonsimilar partial differential equations are transformed into ordinary differential equations by using the difference-differential method. Solutions of resulting equations are expressed in a form of integral equations which are in turn solved by iterative numerical quadratures.

2 Basic equations

We consider a forced and free mixed convection boundary layer flow over a wedge with uniform suction or injection shown in Fig. 1. The boundary layer equations can be written as follows:

$$u\frac{\partial u}{\partial x}+v\frac{\partial u}{\partial y}=\nu\frac{\partial^2 u}{\partial y^2}+U_e\frac{dU_e}{dx}+g\beta(T-T_\infty)\cos\left(\frac{\Omega}{2}\right), \tag{1}$$

$$u\frac{\partial T}{\partial x}+v\frac{\partial T}{\partial y}=\frac{\nu}{\mathrm{Pr}}\frac{\partial^2 T}{\partial y^2}, \tag{2}$$

$$\frac{\partial u}{\partial x}+\frac{\partial v}{\partial y}=0, \tag{3}$$

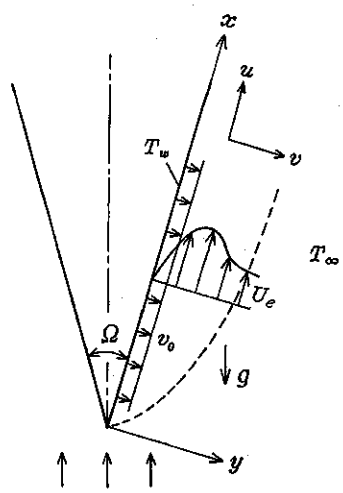

Fig. 1. Schematic diagram of the physical system

with associate boundary conditions,

$$\begin{aligned} &y = 0: \quad u = 0, \quad v = v_0 \text{ (const)}, \quad T = T_w, \\ &y \to \infty: \quad u = U_e(x), \quad T = T_\infty, \end{aligned} \tag{4}$$

where x and y are taken as the coordinates parallel and normal to the wall, respectively. u and v denote the components of fluid velocity in the x and y direction, respectively. T is the temperature, g the gravitational acceleration, ν the kinematic viscosity, β the coefficient of thermal expansion and Pr the Prandtl number. Next, the following set of transformation making use of the stream function will be used:

$$\psi(x, y) = \left(\frac{2}{m+1} \nu x U_e\right)^{1/2} f(x, \eta), \quad \eta = y \left(\frac{m+1}{2} \frac{U_e}{\nu x}\right)^{1/2} \tag{5}$$

$$\theta(x, \eta) = \frac{T - T_\infty}{T_w - T_\infty}. \tag{6}$$

Then the components of the fluid velocity are

$$u = U_e \frac{\partial f}{\partial \eta}, \tag{7}$$

$$v = -\left(\frac{2}{m+1} \frac{\nu U_e}{x}\right)^{1/2} \left(\frac{1}{2} f + \frac{1}{2} \frac{x}{U_e} \frac{dU_e}{dx} f + x \frac{\partial f}{\partial x} + x \frac{\partial f}{\partial \eta} \frac{\partial \eta}{\partial x}\right). \tag{8}$$

Substituting Eqs. (7) and (8) in Eqs. (1) and (2), the following differential equations are obtained:

$$\frac{\partial^3 f}{\partial \eta^3} + f \frac{\partial^2 f}{\partial \eta^2} + \frac{2m}{m+1} \left\{1 - \left(\frac{\partial f}{\partial \eta}\right)^2\right\} + \frac{2}{m+1} A \cdot \theta \cdot \cos\left(\frac{\Omega}{2}\right) = \frac{2}{m+1} x \left(\frac{\partial^2 f}{\partial x \, \partial \eta} - \frac{\partial^2 f}{\partial \eta^2} \frac{\partial f}{\partial x}\right), \tag{9}$$

$$\frac{1}{\mathrm{Pr}} \frac{\partial^2 \theta}{\partial \eta^2} + f \frac{\partial \theta}{\partial \eta} = \frac{2}{m+1} x \left(\frac{\partial f}{\partial \eta} \frac{\partial \theta}{\partial x} - \frac{\partial \theta}{\partial \eta} \frac{\partial f}{\partial x}\right), \tag{10}$$

where A is the buoyancy parameter, Gr the Grashof number and Re the Reynolds number. They are expressed as follows:

$$A = \mathrm{Gr}/\mathrm{Re}^2 = c x^{(1-2m)}, \quad \mathrm{Gr} = g\beta(T_w - T_\infty) \, x^3/\nu^2, \quad \mathrm{Re} = U_e x/\nu. \tag{11}$$

The boundary conditions (4) become

$$\eta = 0: \quad \frac{\partial f}{\partial \eta} = 0, \quad \frac{1}{2} f + \frac{1}{2} \frac{x}{U_e} \frac{dU_e}{dx} f + x \frac{\partial f}{\partial x} = s, \quad \theta = 1,$$
$$\eta \to \infty: \quad \frac{\partial f}{\partial \eta} = 1, \quad \theta = 0, \tag{12}$$

where U_e is the flow velocity at the outer edge of the boundary layer, which is given as $U_e(x) = cx^m$. $m = \gamma/(2-\gamma)$, and γ is the pressure gradient parameter which corresponds to $\gamma = \Omega/\pi$ for a total angle Ω of the wedge. s is the parameter of suction or injection which is defined by

$$s = -v_0 \left(\frac{m+1}{2} \frac{x}{\nu U_e} \right)^{1/2}. \tag{13}$$

Here v_0 is the velocity of suction or injection, when $v_0 < 0$ or $v_0 > 0$, respectively.

For convenience, we put $X = kx^{(1-m)/2}$ ($\equiv s$), then Eqs. (9) and (10) become

$$\frac{\partial^3 f}{\partial \eta^3} + \left(f + \frac{1-m}{1+m} X \frac{\partial f}{\partial X} \right) \frac{\partial^2 f}{\partial \eta^2} + \frac{1-m}{1+m} X \frac{\partial^2 f}{\partial X \, \partial \eta} \frac{\partial f}{\partial \eta}$$
$$+ \frac{2m}{1+m} \left\{ 1 - \left(\frac{\partial f}{\partial \eta} \right)^2 \right\} + \frac{2}{1+m} c \left(\frac{X}{k} \right)^{2(1-2m)/(1-m)} \cdot \theta \cdot \cos \left(\frac{\Omega}{2} \right) = 0, \tag{14}$$

$$\frac{1}{\mathrm{Pr}} \frac{\partial^2 \theta}{\partial \eta^2} + \left(f + \frac{1-m}{1+m} X \frac{\partial f}{\partial X} \right) \frac{\partial \theta}{\partial \eta} - \frac{1-m}{1+m} X \frac{\partial \theta}{\partial X} \frac{\partial f}{\partial \eta} = 0. \tag{15}$$

The boundary conditions (12) are rewritten as

$$\eta = 0: \quad \frac{\partial f}{\partial \eta} = 0, \quad \frac{1}{2}(m+1) f + \frac{1-m}{2} + X \frac{\partial f}{\partial X} = X, \quad \theta = 1,$$
$$\eta \to \infty: \quad \frac{\partial f}{\partial \eta} = 1, \quad \theta = 0. \tag{16}$$

Next, the derivative at $X = X_i = ih$ ($i = 0, 1, 2, \ldots$), where h is a step size of difference, can be approximated by the Gregory-Newton four-point formula as an example. Equations (14) and (15) can be replaced by the ordinary differential equations

$$\frac{d^3 f_i}{d\eta^3} + \left\{ f_i + \frac{i}{6} \frac{1-m}{1+m} (11 f_i - 18 f_{i-1} + 9 f_{i-2} - 2 f_{i-3}) \right\} \frac{d^2 f_i}{d\eta^2}$$
$$- \frac{i}{6} \frac{1-m}{1+m} \left(11 \frac{df_i}{d\eta} - 18 \frac{df_{i-1}}{d\eta} + 9 \frac{df_{i-2}}{d\eta} - 2 \frac{df_{i-3}}{d\eta} \right) \frac{df_i}{d\eta}$$
$$+ \frac{2m}{m+1} \left\{ 1 - \left(\frac{df_i}{d\eta} \right)^2 \right\} + \frac{2}{m+1} c \left(\frac{ih}{k} \right)^{2(1-2m)/(1-m)} \cdot \theta_i \cdot \cos \left(\frac{\Omega}{2} \right) = 0, \tag{17}$$

$$\frac{1}{\mathrm{Pr}} \frac{d^2 \theta_i}{d\eta^2} + \left\{ f_i + \frac{i}{6} \frac{1-m}{1+m} (11 f_i - 18 f_{i-1} + 9 f_{i-2} - 2 f_{i-3}) \right\} \frac{d\theta_i}{d\eta}$$
$$- \frac{i}{6} \frac{1-m}{1+m} (11 \theta_i - 18 \theta_{i-1} + 9 \theta_{i-2} - 2 \theta_{i-3}) \frac{df_i}{d\eta} = 0. \tag{18}$$

The boundary conditions (16) become

$$\eta = 0: \quad \frac{df_i}{d\eta} = 0, \quad f_i = ih, \quad \theta_i = 1,$$
$$\eta \to \infty: \quad \frac{df_i}{d\eta} = 1, \quad \theta_i = 0. \tag{19}$$

We can express the solutions at the i-th station in a form of integral equations as

$$\frac{df_i}{d\eta} = \int_0^\eta E(\eta) \int_0^\eta \frac{R(\eta)}{E(\eta)}\, d\eta\, d\eta + \left\{1 - \int_0^\infty E(\eta) \int_0^\eta \frac{R(\eta)}{E(\eta)}\, d\eta\, d\eta\right\} \frac{G(\eta)}{G(\infty)}, \tag{20}$$

$$f_i = ih + \int_0^\eta \frac{df_i}{d\eta}\, d\eta, \tag{21}$$

$$\theta_i = 1 + \int_0^\eta P(\eta) \int_0^\eta \frac{S(\eta)}{P(\eta)}\, d\eta\, d\eta - \left\{1 + \int_0^\infty P(\eta) \int_0^\eta \frac{S(\eta)}{P(\eta)}\, d\eta\, d\eta\right\} \frac{Q(\eta)}{Q(\infty)}, \tag{22}$$

where

$$E(\eta) = \exp\left[\int_0^\eta \left\{-f_i - \frac{i}{6}\frac{1-m}{1+m}(11f_i - 18f_{i-1} + 9f_{i-2} - 2f_{i-3})\right\} d\eta\right], \tag{23}$$

$$R(\eta) = \frac{i}{6}\frac{1-m}{1+m}\left(11\frac{df_i}{d\eta} - 18\frac{df_{i-1}}{d\eta} + 9\frac{df_{i-2}}{d\eta} - 2\frac{df_{i-3}}{d\eta}\right)\frac{df_i}{d\eta} - \frac{2m}{m+1}\left\{1 - \left(\frac{df_i}{d\eta}\right)^2\right\} - \frac{2}{m+1}\, c\left(\frac{ih}{k}\right)^{2(1-2m)/(1-m)} \cdot \theta_i \cdot \cos\left(\frac{\Omega}{2}\right), \tag{24}$$

$$G(\eta) = \int_0^\eta E(\eta)\, d\eta, \tag{25}$$

Fig. 2. Velocity profiles for Pr = 0.73, $A = 1.0$ and $m = 0.0909$. **Fig. 3.** Temperature profiles for Pr = 0.73, $A = 1.0$ and $m = 0.0909$. **Fig. 4.** Relation between the maximum velocity U_{max} and suction/injection parameter s for Pr = 0.73 and $m = 0.0909$. **Fig. 5.** Relation between the position η_m of maximum velocity and suction/injection parameter s for Pr = 0.73 and $m = 0.0909$. **Fig. 6.** Velocity profiles for Pr = 0.73 and $A = 1.0$. **Fig. 7.** Velocity profiles for $A = 1.0$ and $m = 0.0909$

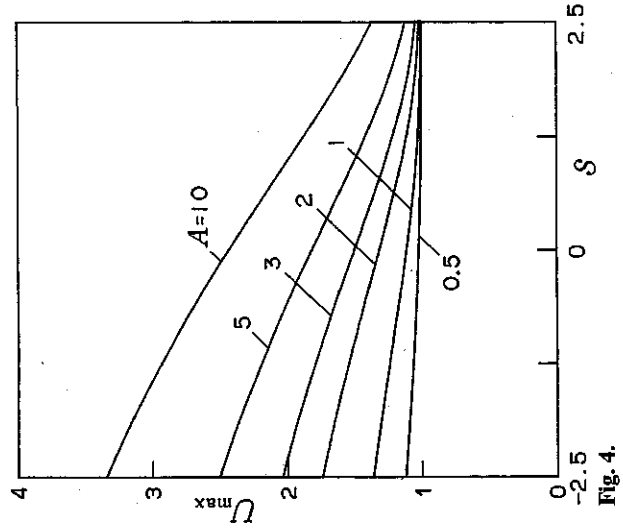

Fig. 4.

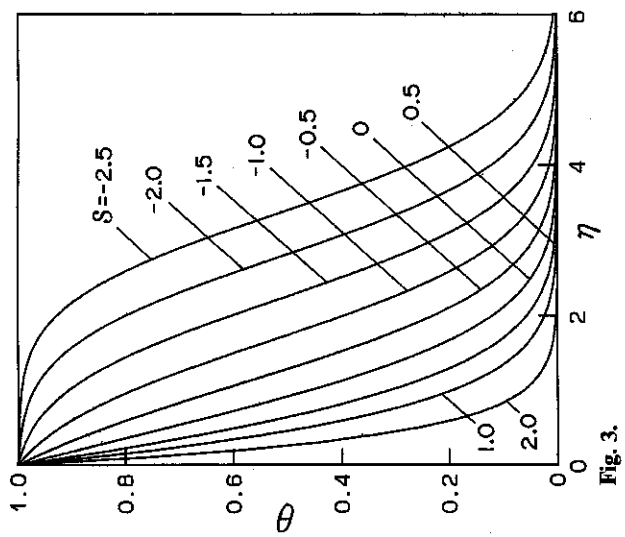

Fig. 3.

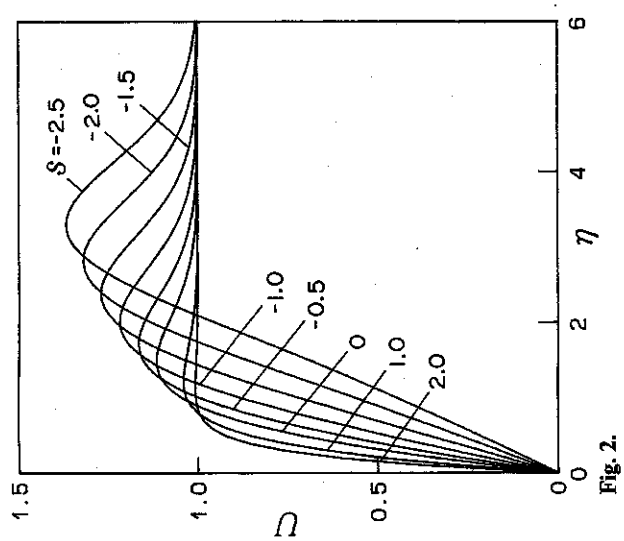

Fig. 2.

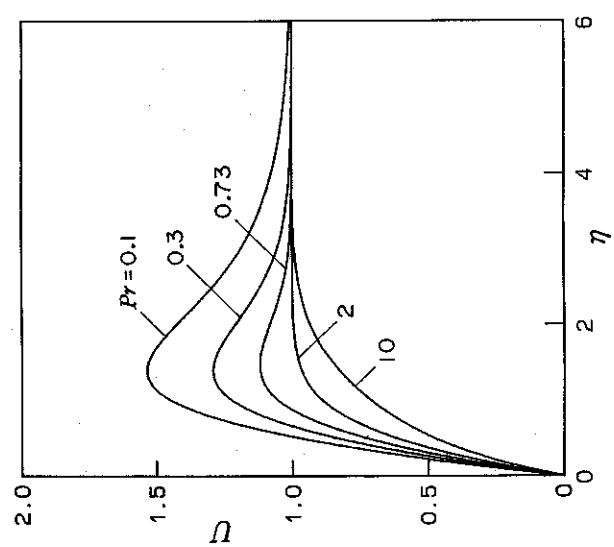

Fig. 7.

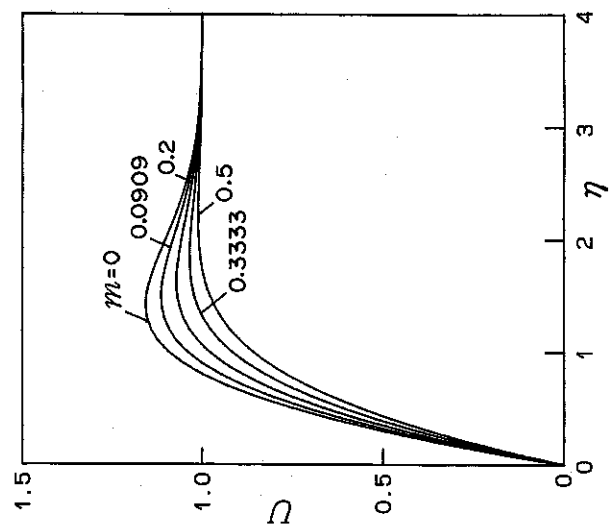

Fig. 6.

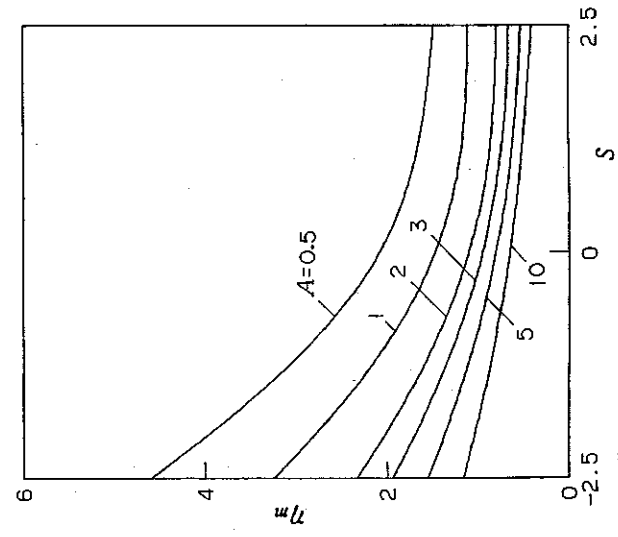

Fig. 5.

$$P(\eta) = \exp\left[\int_0^\eta \left\{-\mathrm{Pr}\cdot f_i - \frac{i\,\mathrm{Pr}}{6}\frac{1-m}{1+m}(11f_i - 18f_{i-1} + 9f_{i-2} - 2f_{i-3})\right\} d\eta\right], \tag{26}$$

$$Q(\eta) = \int_0^\eta P(\eta)\, d\eta, \tag{27}$$

$$S(\eta) = \frac{i\,\mathrm{Pr}}{6}\frac{1-m}{1+m}\left(11\theta_i - 18\theta_{i-1} + 9\theta_{i-2} - 2\theta_{i-3}\right)\frac{df_i}{d\eta}. \tag{28}$$

Iterative numerical quadratures of integral equations (20), (21) and (22) are carried out using a Simpson's numerical integration scheme. The solutions at the station $X = X_i$ can be determined when the variable quantities at all previous stations $X = X_{i-1}$, X_{i-2} and X_{i-3} are known. The functions $f_0(\eta)$ and $\theta_0(\eta)$ at $X = X_0$ are the values of $X = 0$ ($x \neq 0$), which means the suction velocity $v_0 = 0$. The derivative with respect to X in Eqs. (14) and (15) disappears and the solutions $f_0(\eta)$ and $\theta_0(\eta)$ at the station $X = 0$ are calculated easily. The functions at $X = X_1$ and $X = X_2$ can be obtained by using a two-point and three-point formula instead of four point formula. The numerical calculations are proceeded to $s > 0$ or $s < 0$, respectively. The solutions are considered to have been obtained when the difference of two successive iterative values of $d^2f/d\eta^2$ and $d\theta/d\eta$ at $\eta = 0$ become less than a criterion of convergence. The criterion of convergence in the iteration is set equal to 5×10^{-7}.

3 Numerical results and discussions

Iterative numerical quadratures are carried out for various values of the suction/injection parameter s, buoyancy parameter A, Prandtl number Pr and the pressure gradient parameter m.

Figures 2 and 3 represent the velocity profiles $U(= u/U_e)$ and the temperature profiles θ, for pressure gradient parameter $m = 0.0909$ ($\Omega = 30°$), buoyancy parameter $A = 1.0$ and Prandtl number $\mathrm{Pr} = 0.73$, as a function of suction or injection parameter s, respectively. With a decrease in the suction parameter s, which corresponds to either increasing injection or decreasing suction, the temperature profiles swell. On the other hand, as the parameter s is decreased, the maximum velocity $U_{\max}$ increases, and the location η_m of maximum velocity increases and shifts away from the wall. The relations $U_{\max}$, η_m versus the suction/injection parameter s are illustrated in Figs. 4 and 5.

Complementary to the previous figures, velocity profiles and the temperature profiles for $s = 0$ are depicted in Figs. 6 to 11. Figure 6 shows the velocity profiles for a pressure gradient parameter $m = 0$ ($\Omega = 0°$), 0.0909 (30°), 0.2 (60°), 0.3333 (90°), and 0.5 (120°) at Prandtl number $\mathrm{Pr} = 0.73$ and buoyancy parameter $A = 1.0$. Figure 7 is for $m = 0.0909$ and $A = 1.0$, and Prandtl number Pr as parameter, where Fig. 8 is for $m = 0.0909$ and $\mathrm{Pr} = 0.73$, and the buoyancy

Fig. 8. Velocity profiles for $\mathrm{Pr} = 0.73$ and $m = 0.0909$. **Fig. 9.** Temperature profiles for $\mathrm{Pr} = 0.73$ and $A = 1.0$. **Fig. 10.** Temperature profiles for $A = 1.0$ and $m = 0.0909$. **Fig. 11.** Temperature profiles for $\mathrm{Pr} = 0.73$ and $m = 0.0909$. **Fig. 12.** Relation between skin friction parameter $f''(0)$ and suction/injection parameter s for $\mathrm{Pr} = 0.73$ and $m = 0.0909$. **Fig. 13.** Relation between the heat transfer parameter $\theta'(0)$ and suction/injection parameter s for $\mathrm{Pr} = 0.73$ and $m = 0.0909$

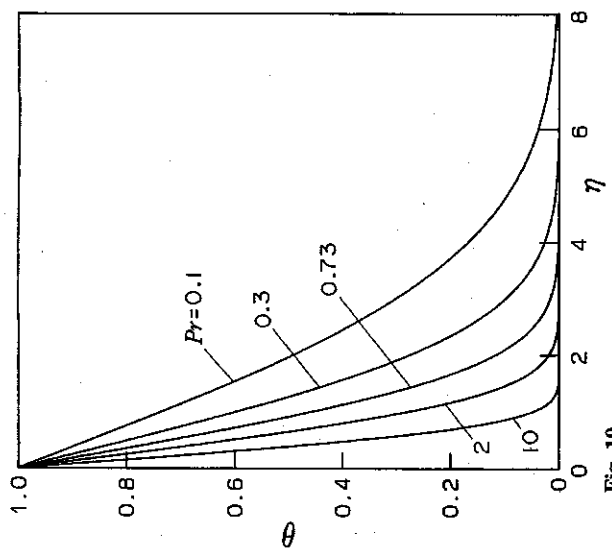

Fig. 10.

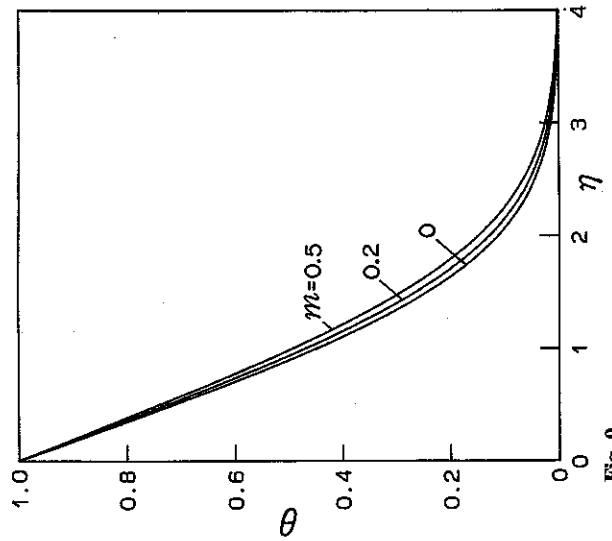

Fig. 9.

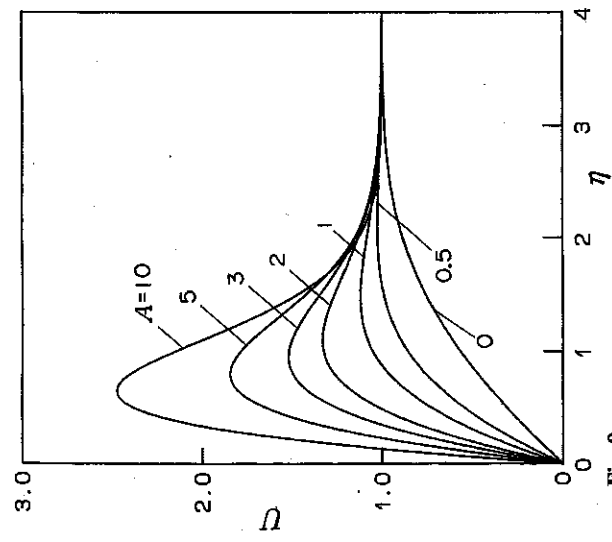

Fig. 8.

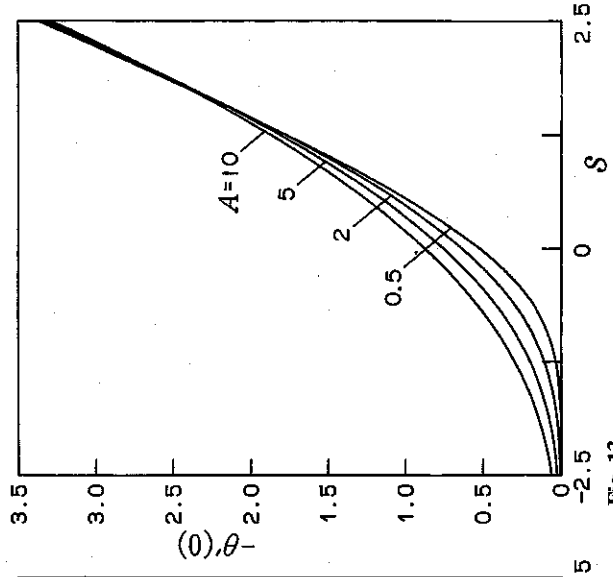

Fig. 13.

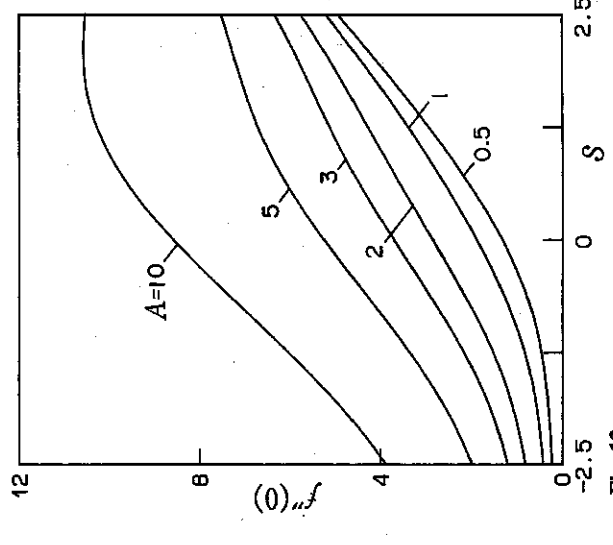

Fig. 12.

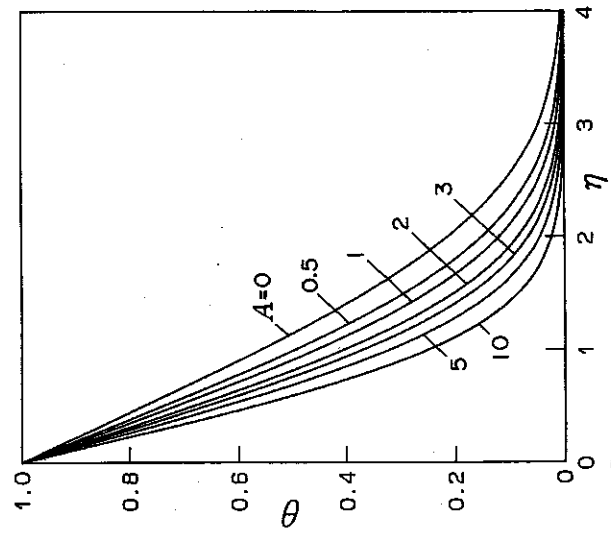

Fig. 11.

parameter A as parameter. With a decrease in m and Pr, and an increase in A, the maximum velocity U_{max} increases. With an increase of m and Pr, and decrease of A, the location η_m of maximum velocity increases and shifts away from the wall. On the other hand, temperature profiles θ for $s = 0$ are illustrated in Figs. 9 to 11.

Figure 9 represents the results for $Pr = 0.73$ and $A = 1.0$, and the pressure gradient parameter m as parameter, where Fig. 10 is for $m = 0.0909$ and $A = 1.0$, and the Prandtl number Pr as parameter. Figure 11 is for $m = 0.0909$ and $Pr = 0.73$, and the buoyancy parameter A as parameter. With an increase in the pressure gradient parameter m, and a decrease in Prandtl number Pr and buoyancy parameter A, the temperature profiles swell.

The skin friction and heat transfer coefficients $f''(0)$ and $\theta'(0)$ are shown in Tables 1, 2 and Figs. 12, 13. Table 1 presents the $f''(0)$ and $\theta'(0)$ for $Pr = 0.73$, $m = 0.0909$, $A = 1$ and various values of s. Figures 12 and 13 show the $f''(0)$ and $\theta'(0)$ versus the suction/injection parameter s for various values of the buoyancy parameter A at $Pr = 0.73$ and $m = 0.0909$, respectively. It is seen that the skin friction and heat transfer parameters increase with increasing s, which corresponds to either an increasing suction or a decreasing injection. Further, Table 2 presents the values of $f''(0)$ and $\theta'(0)$ for various values of m and A. This Table shows that the skin friction and heat transfer parameters increase when A increases and m decreases.

The physical reasons for the behavior of the skin friction and heat transfer parameters in Table 1 are easily deduced from Figs. 2 and 3.

Table 1. Values of $f''(0)$ and $\theta'(0)$ for $Pr = 0.73$, $m = 0.0909$ and $A = 1.0$

s	$f''(0)$	$-\theta'(0)$
−2.5	0.42558	0.00095
−2.0	0.53488	0.00697
−1.5	0.70991	0.03362
−1.0	0.98579	0.11265
−0.5	1.37927	0.28175
0.0	1.87405	0.56590
0.5	2.43933	0.96952
1.0	3.05506	1.47859
1.5	3.71904	2.06640
2.0	4.43591	2.70217
2.5	5.20427	3.36068

Table 2. Values of $f''(0)$ and $\theta'(0)$ for $Pr = 0.73$ and $s = 0$

	$A = 0.0$		0.5		1.0		5.0	
m	$f''(0)$	$-\theta'(0)$	$f''(0)$	$-\theta'(0)$	$f''(0)$	$-\theta'(0)$	$f''(0)$	$-\theta'(0)$
0.0	0.46960	0.42015	1.30573	0.52043	1.96409	0.57649	5.84177	0.78272
0.0435	0.56898	0.43548	1.31654	0.52018	1.92595	0.57164	5.57042	0.76837
0.0909	0.65498	0.44730	1.31804	0.51915	1.87405	0.56590	5.25094	0.75198
0.1429	0.73200	0.45693	1.31250	0.51757	1.81142	0.55949	4.89123	0.73363
0.2	0.80213	0.46503	1.30189	0.51564	1.74111	0.55259	4.50044	0.71350
0.3333	0.92765	0.47814	1.27303	0.51135	1.58902	0.53814	3.65775	0.66822
0.5	1.03890	0.48848	1.24500	0.50747	1.44040	0.52416	2.78869	0.61708

4 Conclusions

The present paper is a contribution to the analysis of mixed convection flow with uniform suction or injection on a wedge. The ordinary differential equations were obtained by means of a difference-differential method. The solutions of the resulting equations are performed by integral ones, and the boundary layer characteristics are given by calculating the solutions.

Acknowledgement

The authors wish to express their hearty thanks to Prof. R. Kobayashi, Tohoku University, for guidance and encouragement.

References

[1] Sparrow, E. M., Eichorn, R., Gregg, J. C.: Combined forced and free convection in a boundary layer flow. Phys. Fluids **2**, 319–328 (1959).
[2] Szewczyk, A. A.: Combined forced and free-convection laminar flow. Trans. ASME Ser. C **86**, 501–507 (1964).
[3] Lloyd, J. R., Sparrow, E. M.: Combined forced and free convection flow on vertical surfaces. Int. J. Heat Mass Transfer **13**, 434–438 (1970).
[4] Mucogh, A., Chen, T. S.: Analysis of combined forced and free convection across a horizontal cylinder. Can. J. Chem. Eng. **55**, 265–271 (1977).
[5] Rajn, M. S., Liu, X. R., Law, C. K.: A formulation of combined forced and free convection past horizontal and vertical surfaces. Int. J. Heat Mass Transfer **27**, 2215–2224 (1984).
[6] Wang, T.-Y., Kleinstreuer, C.: Combined free-forced convection heat transfer between vertical slender cylinders and power-law fluids. Int. J. Heat Mass Transfer **31**, 91–98 (1988).
[7] Lee, S. L., Hsu, K.: Interaction of surface suction/blowing with buoyancy force on mixed convection flow adjacent to an inclined flat plate. Int. J. Heat Mass Transfer **32**, 1989–1991 (1989).
[8] Wang, T.-Y., Kleinstreuer, C.: Mixed thermal convection of power-law fluids past bodies with uniform fluid injection or suction. ASME J. Heat Transfer **112**, 151–156 (1990).
[9] Watanabe, T.: Forced and free mixed convection boundary layer flow with uniform suction or injection on a vertical flat plate. Acta Mech. **89**, 123–132 (1991).

Authors' address: Prof. T. Watanabe, Assoc. Prof. K. Funazaki, and Grad. stud. H. Taniguchi, Department of Mechanical Engineering, Faculty of Engineering, Iwate University, Morioka 020, Japan